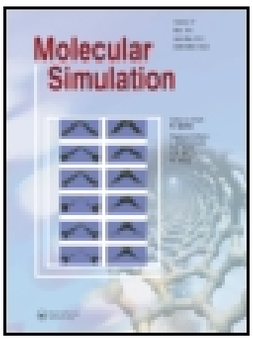

Molecular Simulation

ISSN: (Print) (Online) Journal homepage: https://www.tandfonline.com/loi/gmos20

Layer-based thermal migration of an ionic liquid nano-droplet on a graphene surface: a molecular dynamics study

Jingqiu Wang , Yong Zhang , Xiaolei Wang & Edward J. Maginn

To cite this article: Jingqiu Wang , Yong Zhang , Xiaolei Wang & Edward J. Maginn (2020): Layer-based thermal migration of an ionic liquid nano-droplet on a graphene surface: a molecular dynamics study, Molecular Simulation

To link to this article: https://doi.org/10.1080/08927022.2020.1776277

Published online: 12 Jun 2020.

MOLECULAR SIMULATION
https://doi.org/10.1080/08927022.2020.1776277

Taylor & Francis
Taylor & Francis Group

Layer-based thermal migration of an ionic liquid nano-droplet on a graphene surface: a molecular dynamics study

Jingqiu Wang [a,b], Yong Zhang [b], Xiaolei Wang [a] and Edward J. Maginn [b]

[a]College of Mechanical and Electrical Engineering, Nanjing University of Aeronautics and Astronautics, Nanjing, People's Republic of China; [b]Department of Chemical and Biomolecular Engineering, University of Notre Dame, Notre Dame, IN, USA

ABSTRACT

The migration behaviour of an ionic liquid (IL) nano-droplet on a graphene surface under temperature gradients was studied using non-equilibrium molecular dynamics (MD) simulations. 1-ethyl-3-methylimidazolium tetrafluoroborate ([EMIM][BF4]) was used in the study. The migration of the IL nano-droplet from the hot end to the cold end of the graphene surface was observed under all temperature gradients considered in the current work. The migration was found to be faster under higher temperature gradients. Detailed analysis reveals that, instead of rolling like a ball, the IL nano-droplet migrates via a layer-based motion, in which the molecules have limited displacement in the direction perpendicular to the graphene surface. The migration of the IL nano-droplet was also found to be coupled with spreading on the graphene surface. The spatial organisation of the cations and anions within the IL nano-droplet was also analysed. It was found that the ions forming the IL nano-droplet organised themselves in layers parallel to the graphene surface, and the angles of cation rings on different layers also tend to be specific. The cation closest to the graphene surface tends to align with their rings parallel to the surface, while those away from the surface are more disordered.

ARTICLE HISTORY
Received 5 February 2020
Accepted 26 May 2020

KEYWORDS
Thermal migration; temperature gradient; ionic liquid nano-droplets; graphene surface

1. Introduction

Thermal migration, a phenomenon where a liquid on a substrate flows from a high-temperature area to a low-temperature area, plays a key role in many applications such as the lubrication of machines working under wide temperature variation [1,2] and in microfluidic devices [3–5]. Many theoretical and experimental efforts have been devoted to understand the mechanisms and to find the dominant factors of thermal migration [6,7]. It has been found that besides the temperature gradient [8] as the driving force, surface topography and texture [9–11], surface energy [5], additives [12], substrate materials [4] and liquid type [13,14] can also greatly influence the migration behaviour.

It is only recently that the thermal migration phenomenon has been studied using molecular dynamics (MD) simulations. MD simulations are an effective means to provide the view of liquid movement at the molecular level. Using non-equilibrium MD simulations, Becton and Wang [15] explored the feasibility of utilising a thermal gradient to control the motion of a small graphene nano-flake on a large graphene substrate. Lohrasebi et al. [16] found that the free energy decreases as a C60 molecule moves from the hot end toward the cold end of a graphene sheet. Recently, Foroutan et al. [17] studied the effect of temperature gradient on the behaviour of a water nano-droplet resting on suspended graphene. They confirmed that the droplet is driven to the cold end by the applied temperature gradient. Similarly, an MD simulation study of the transport of an ionic liquid (IL) droplet in a carbon nanotube subjected to a thermal gradient has been reported [14]. The droplet drifted along the axis of the nanotube toward the lower temperature region. Simulations have also been carried out to study the temperature effects on spreading of water nano-droplets on a polymer surface [18].

ILs are low-temperature molten salts that generally combine bulky asymmetric cations with various anions. Most of the distinctive physical and chemical properties of ILs, such as good thermal stability, low volatility and reasonable viscosity-temperature behaviour are in line with the desired performance of lubricants, giving them the potential to become high-performance lubricants that can be used under harsh conditions such as those encountered in the field of aerospace engineering. Various experimental studies [19,20] considering ILs as lubricants have been performed. It was found that some IL lubricants have excellent anti-wear and anti-friction properties, and the tribological properties were superior to traditional lubricants. Particularly, Huang et al. [21] studied in experiments the migration behaviour of an ionic liquid droplet on a stainless steel surface under a temperature gradient. Unlike molecular lubricating oil, the IL droplet did not migrate under the experimental conditions. It was hypothesised that this abnormal behaviour originated from a combination of ordering structure of ions at the interfaces as well as the Coulombic interactions inside the droplet.

In the present study, we performed MD simulations of IL nano-droplet migration on a graphene surface under varying temperature gradients. To achieve a good understanding of the thermal migration of the IL nano-droplet, the changes in velocity of the IL nano-droplet during the migration were

CONTACT Edward J. Maginn ed@nd.edu

analysed. Molecular structure in terms of density profile and cation orientation were also analysed.

2. Methodology

The simulation system consisted of an IL nano-droplet on a graphene surface, as shown in Figure 1(a). 1-ethyl-3-methylimidazolium tetrafluoroborate ([EMIM][BF4]) was used in the current study, as it is well studied and is commercially available. The nano-droplet consisted of 65 ion pairs, which yielded a nano-droplet diameter of about 3 nm. The single-layer graphene surface had dimensions of $L_x \times L_y$=40 nm × 50 nm, as shown in Figure 1(b), which has 76,936 carbon atoms. The simulation system was put in a box with the size of 40 nm × 50 nm × 10 nm. Periodic boundary conditions were applied in all three directions. Initially, the IL nano-droplet was placed at the centre in the *X* direction, 5 nm to the left (hot) end and 0.5 nm above the graphene sheet.

To prepare the system, the IL was equilibrated at 300 K for 2 ns, during which the centre of mass (COM) of the nano-droplet was fixed. For the graphene surface, atoms in the first 1 nm on both ends along the *Y*-direction were fixed during the simulation. Atoms of the next 4 nm were coupled with a Nosé–Hoover thermostat with damping coefficient of 0.1 ps^{-1}. The temperature of the cold end (T_C) of the graphene surface was kept at 300 K throughout the simulation, while the hot end has a higher temperature (T_H) of 350, 400, 450 and500 K, to obtain a temperature gradient of 1.25, 2.5, 3.75, 5 K/nm, respectively. At the end of the equilibration, the temperature distribution of the graphene surface was computed, as shown in Figure 2. After the system was equilibrated, the constraint applied to the COM of the IL droplet was removed and the IL droplet was allowed to evolve in a NVE ensemble for 2.5 ns.

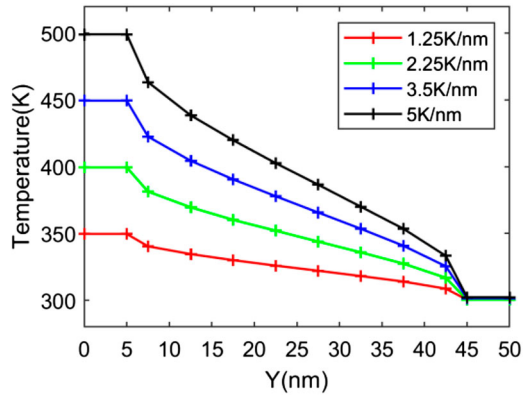

Figure 2. (Colour online) The equilibrated temperatures of the graphene surface before adding the IL droplet under different temperature gradients.

MD simulations were performed using the LAMMPS [22] package with a timestep of 1 fs. [EMIM][BF4] was described using the general Amber force field (GAFF) [23] with the partial atomic charges derived using the RESP [24] method for each isolated ion in the vacuum at the B3LYP/6-311++G(d,p) level using Gaussian09 [25]. The atoms in the graphene surface were modelled by the adaptive intermolecular reactive empirical bond order potential (AIREBO) [26]. The Lorentz–Berthelot mixing rule was used to model the interactions between IL and the graphene surface. Three independent simulations were carried out at the same temperatures under each temperature gradient with different random seeds for initial velocity generation. Averages were computed from these independent simulations.

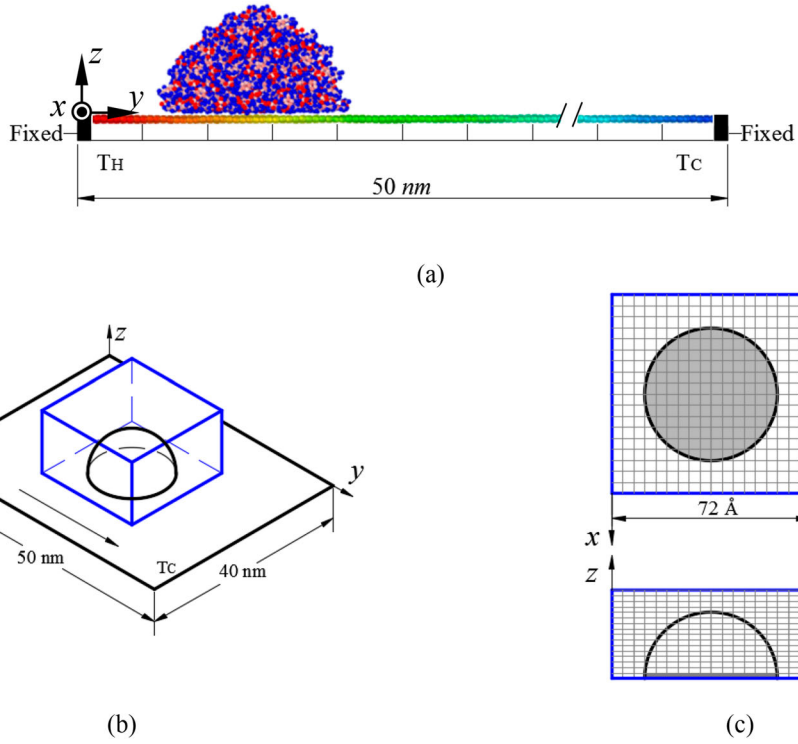

Figure 1. (Colour online) (a) Schematic of the simulation system. (b) 3D schematic of the calculation domain. (c) Two schematic views of the calculation domain and bins.

To analyse the results, the bounding box method reported previously [27] was adopted. The coordinates of the COM of the droplet were calculated at each time step. Based on the calculated COM, abounding box of size 72 Å × 72 Å × 30 Å was obtained. The bounding box was then divided into 36 Å × 36 Å × 30 Å bins as schematically shown in Figure 1(c). By counting the number of particles in each bin, the number density and charge density of the IL droplet was determined.

3. Results and discussion

3.1. Migration of nano-droplet

In the simulation, the IL nano-droplet migration was observed under all the studied temperature gradients. Under the smallest temperature gradient, the IL nano-droplet travelled half way along the *Y*-direction of the graphene surface in 2.5 ns. Under all the other temperature gradients, the nano-droplet reached the cold end of the surface within the 2.5 ns simulation. The migration behaviour under each temperature gradient was analysed based on the first trip from the hot end to the cold end.

Figure 3(a) shows the temperature of the IL nano-droplet during the migration under different temperature gradients. The average temperature of the IL nano-droplet falls to around 200 K when it first lands on the graphene surface due to the exchange of kinetic and potential energies. The temperature then quickly increases and reaches a maximum, and then decreases as the nano-droplet migrates across the surface. It was found that the temperature of the nano-droplet increases faster under a larger temperature gradient and the highest average temperatures of the IL nano-droplet are greater under higher temperature gradients than those under lower temperature gradients. As shown in Figure 3(b), the IL nano-droplet moves faster on the surface with the largest temperature gradient. It took only 0.7 and 1.5 ns for the nano-droplet to travel from the hot end to the cold end under temperature gradients of 5 and 3.75 K/nm, respectively. Under a 1.25 K/nm temperature gradient, the nano-droplet travelled less than 32 nm during the 2.5 ns simulation time. The instantaneous velocities of the IL nano-droplet COM along the *Y*-direction are shown in Figure 3(c). As expected, the highest average velocity was observed under the largest temperature gradient, which has a value of 0.057 nm/ps.

To further study the migration behaviour, the trajectories of three atoms of an ion initially located at the top layer, middle layer and bottom layer of the IL nano-droplet were tracked. Two cations and an anion were chosen randomly. The 3D trajectories of an atom of each ion under temperature gradient 1.25 K/nm are shown in Figure 4 in magenta (top layer), green (middle layer) and blue (bottom layer), respectively. Trajectories of other atoms in each ion are shown in grey. It can be seen from the figure that all three atoms move mainly along the

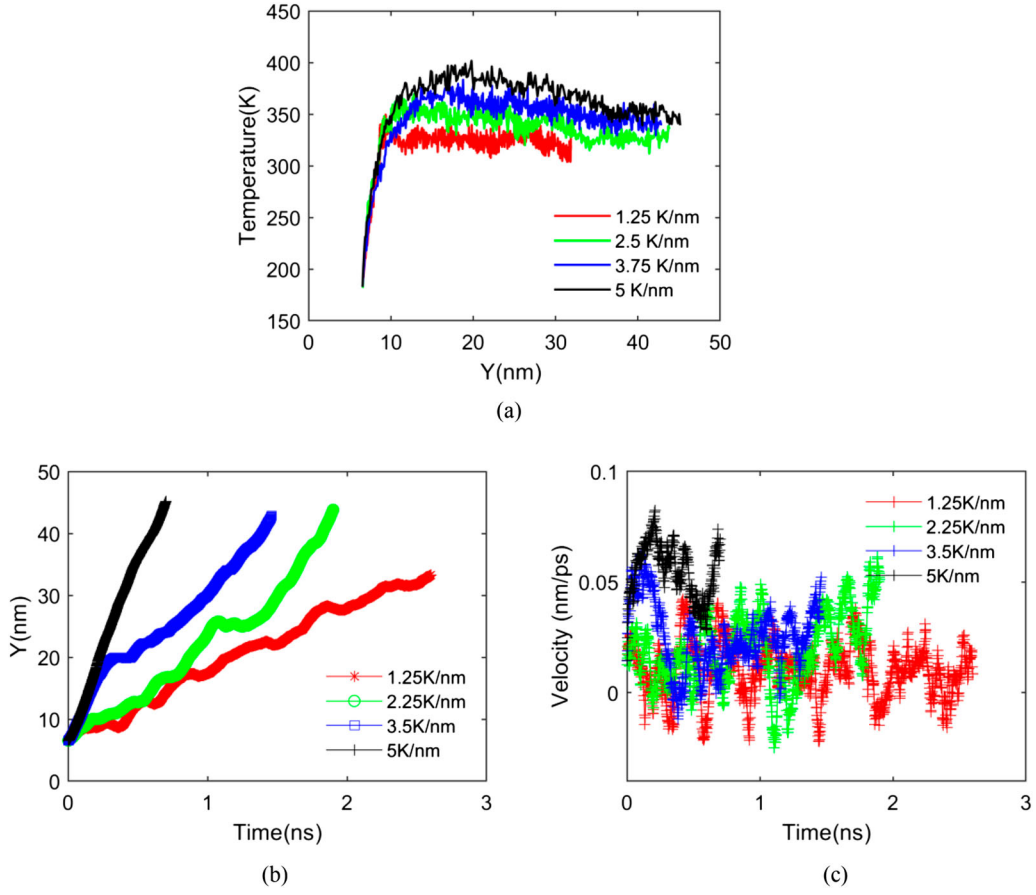

Figure 3. (Colour online) IL nano-droplet migration under different temperature gradients. (a) Average temperature of the IL droplet as a function of temperature gradient. (b) COM position of the IL droplet in *Y*-direction as a function of simulation time. (c) The instantaneous COM velocity of the IL nano-droplet in the *Y*-direction as a function of temperature gradient.

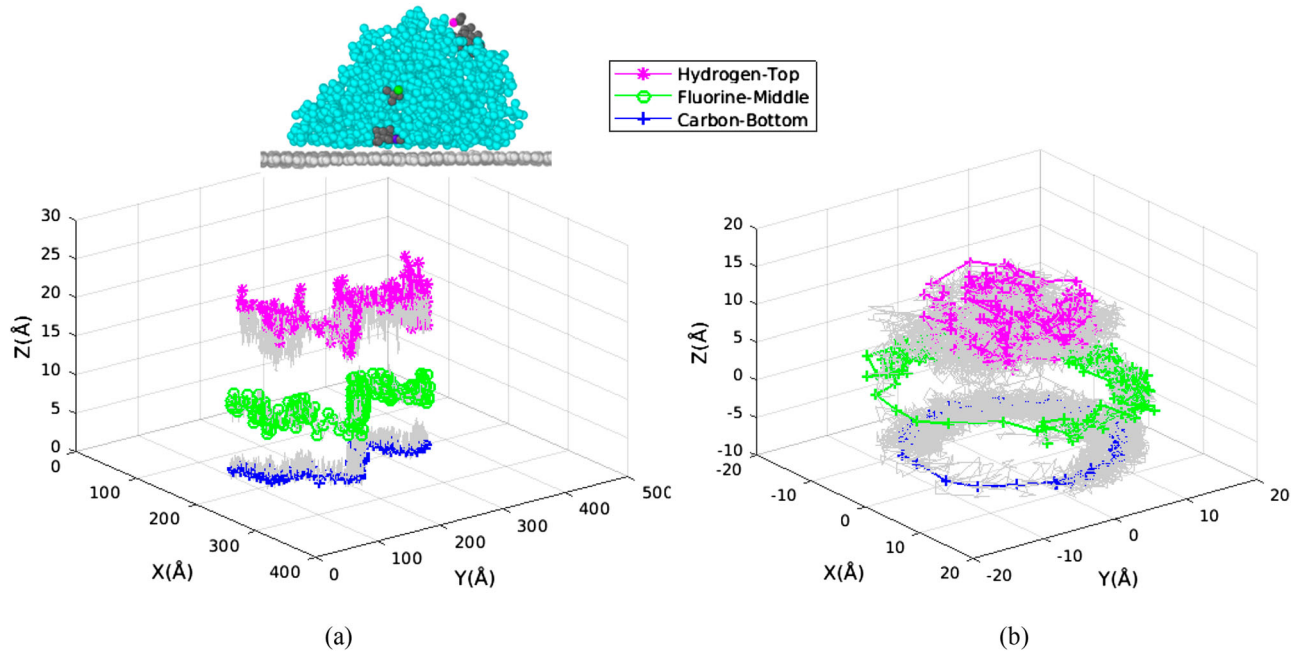

Figure 4. (Colour online) (a) Trajectory of three ions. The initial position of the three chosen atoms of the ions are shown in the inset. (b) Movement of three ions relative to the IL nano-droplet COM.

Y-direction, the direction of temperature gradient, with some random movement in the *X*-direction. The displacement in the *Z*-direction (perpendicular to the surface) is very limited. This migration behaviour is clearer in Figure 4(b) where the movement of the selected atoms relative to the nano-droplet COM is provided. It can be seen that the three ions spin around the vertical axis (*Z*-direction) during the simulation without much displacement in the *Z*-direction. Note that, however, due to the lack of driving force in the *X*-direction, the spin direction is random and keeps changing while the droplet migrates along *Y*-direction.

The movement of IL nano-droplet ions in the *Z*-direction was further studied quantitatively. The maximum displacement in the *Z*-direction (ΔZmax) during the simulation was calculated for each ion and the results are shown in Figure 5(a). It was found that 80% of IL ions moved less than 7 Å in the *Z*-direction during the simulation, and half of the ions moved even less than 5 Å. For the ions at the bottom ($Z \leq 5$ Å) of the nano-droplet, the maximum displacements are even smaller. As shown in Figure 5 (b), 85% of these ions moved less than 3 Å in the *Z*-direction during the simulation, suggesting strong interactions between the IL nano-droplet ions and the graphene surface. This observation suggests that most ions do not switch layers in the *Z*-direction while migrating along the temperature gradient. The same behaviour was also observed for all the ions under all temperature gradients. This behaviour is similar to 'laminar flow' where fluid particles close to a solid surface move in straight lines parallel to the surface without disruption between layers, which usually happens at low Reynolds number [28].

During the migration, the geometry of the IL nano-droplet changes. Figure 6(a) shows the dimensions of the IL nano-droplet in the *X*, *Y* and *Z*-directions, respectively, as a function of simulation time under a temperature gradient of 3.75 K/nm. During the migration, the width (*X*-direction) and length (*Y*-

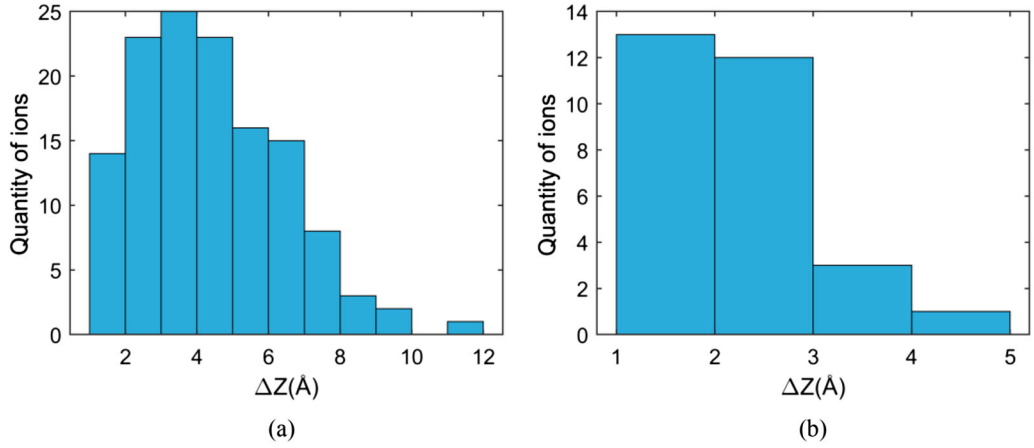

Figure 5. (Colour online) (a) Distribution of ΔZmax of all ions of IL nano-droplet. (b) Distribution of ΔZmax of ions at the bottom layers ($Z \leq 5$ Å) of the nano-droplet.

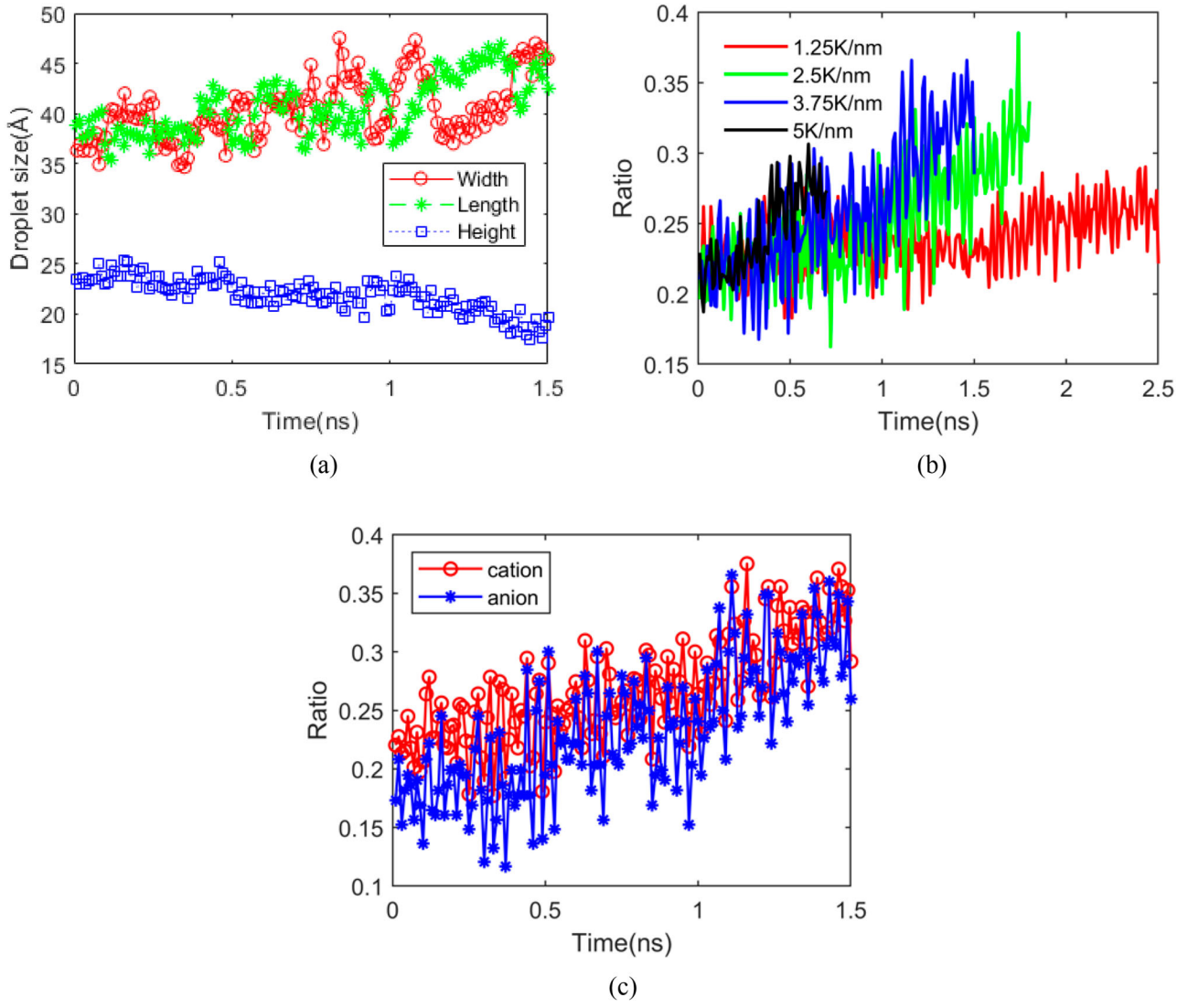

Figure 6. (Colour online) (a) Geometrical change of the IL nano-droplet as a function of simulation time under temperature gradient 3.75 K/nm. (b) Ratio of number of ions in the bottom layer of the IL nano-droplet to that of ions in the rest of the nano-droplet at each temperature gradient. (c) Ratio of ions in the bottom layer to that in the rest of the nano-droplet calculated for cations and anions, respectively, under temperature gradient 3.75 K/nm.

direction) of the IL nano-droplet, calculated based on the bottom layer, increases whereas the height (Z-direction) decreases. This clearly suggests that the nano-droplet 'flattens' during thermal migration. Figure 6(b) shows the ratio of ion numbers in the bottom layer to the number in the rest of the IL nano-droplet under different temperature gradients. This ratio increases faster under a larger temperature gradient. Figure 6(c) shows the same ratio calculated for cations and anions, respectively, under a 3.75 K/nm temperature gradient. While the ratios of both cation and anion increase during the droplet migration, the ratio for the cation is almost always slightly higher than that for anion, which suggests that there are more cations than anions in the bottom layer of the IL nano-droplet.

3.2. Structure of IL nano-droplet

The structure of the IL nano-droplet on the graphene surface was also studied. Figure 7(a) shows the positions of the COM of each IL ion projected onto the Y–Z plane under the temperature gradient 1.25 K/nm. A distinct layered distribution of the ions can be observed. The corresponding number density profile was calculated and is shown in Figure 7(b). The first peak in the profile at about 5 Å from the graphene surface can be seen for both cations and anions, and the peaks at longer distances are relatively lower, suggesting a preferred distribution of both cation and anion at the surface. It can also be seen that the first anion peak shows up at a slightly longer distance from the surface than that of the cation. This behaviour can be more easily seen in Figure 7(c) where the ratio of the cation and anion number density is provided. At a distance of 3 Å, the ratio reaches its maximum of 5, suggesting the number of cations are five times that of anions at the graphene surface. The results under other temperature gradients are similar. The preferred distribution of the cation at the graphene surface observed in the current work is similar with studies reported previously [29,30].

Similarly, the charge density profile as a function of distance from the graphene surface was also calculated and the results under a temperature gradient of 1.25 K/nm are shown in Figure 8(a). Figure 8(b) shows the contribution from the cation and

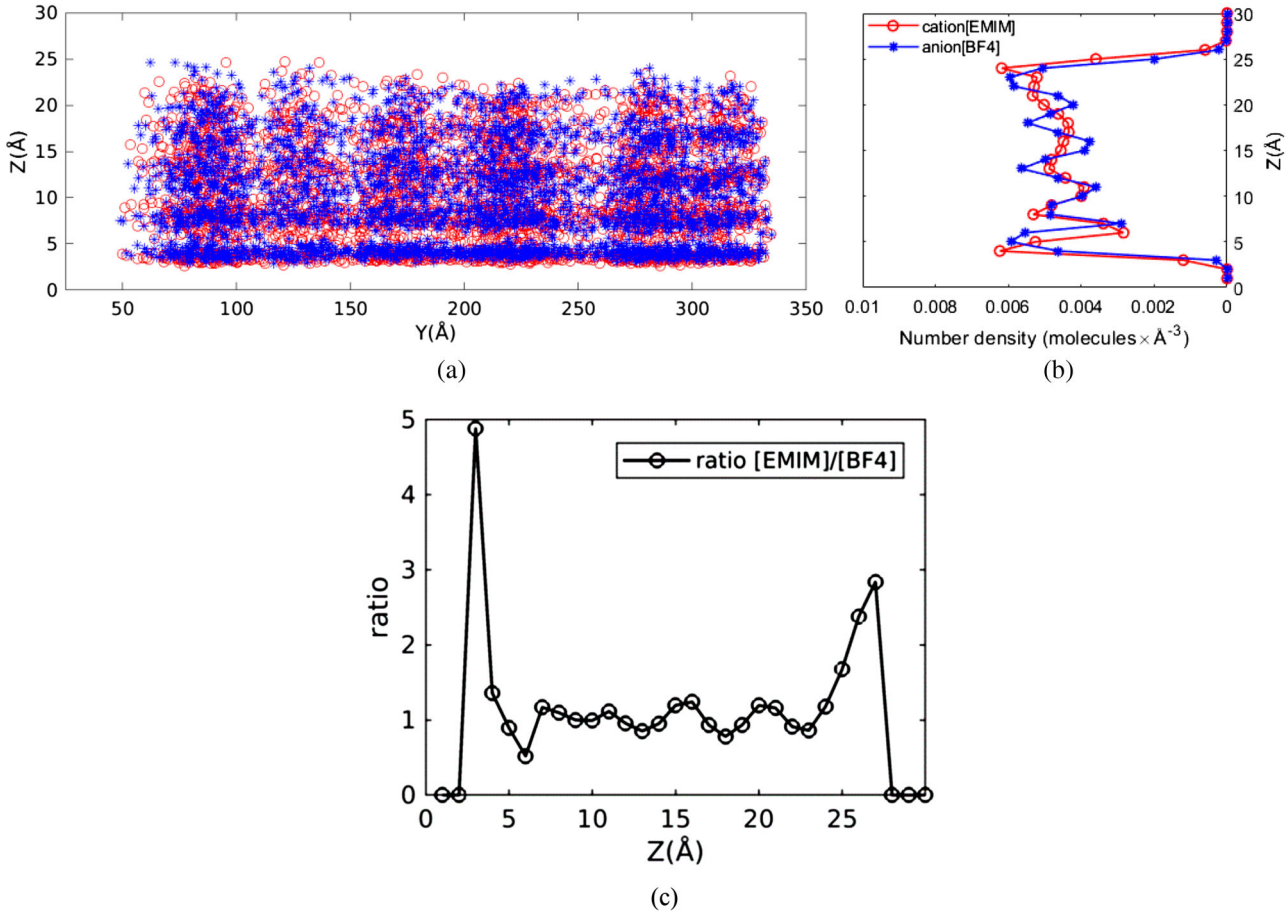

Figure 7. (Colour online) (a) Projection of COM of all molecules on the *Y*–*Z* plane. (b) Number density distribution of IL ions. (c) Ratio of cation to anion number density of IL nano-droplet on graphene surface along the *z*-axis. Results are for a temperature gradient of 1.25 K/nm.

anion, respectively. Note that these charge density profiles were calculated based on atom positions, not COM of the ions. Consistent with the number density profile, a layered distribution of charges can be observed in Figure 8. This layered distribution is more obvious when it is close to the graphene surface. At a distance of 5 Å from the surface, the charge density profile shows a maximum of about 0.0048 e/Å^3. The positive charge at the surface is consistent with the finding the cation density is enriched near the graphene surface.

Finally, the orientation of the cations were studied. An order parameter was defined as

$$S_\theta = \left(\frac{1}{2}(3\sin^2\theta - 1)\right), \tag{1}$$

where θ is the angle between the plane of the cation ring and the graphene surface. The order parameter S_θ has a value of −0.5 if the cation ring is parallel to the graphene surface and a value of

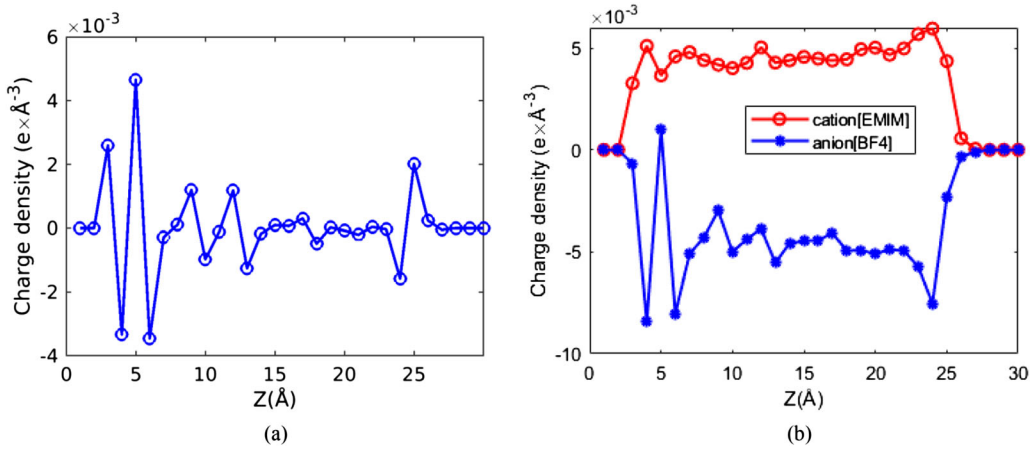

Figure 8. (Colour online) (a) Charge distribution of IL nano-droplets on graphene surface as a function of distance from the graphene surface. (b) Charge distribution calculated for cations and anions, respectively, as a function of distance from the graphene surface. Results are for a temperature gradient of 1.25 K/nm.

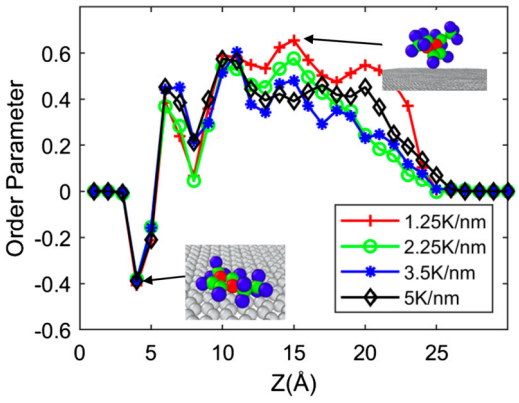

Figure 9. (Colour online) Order parameter calculated for the dihedral angle between the cation ring and the graphene surface at different temperature gradients. Colour code for the molecular structures shown in the inset is as follows: hydrogen atoms in blue, carbon atoms (cation) in green, nitrogen atoms in red, carbon atoms (graphene) in light gray.

1.0 if the cation ring is perpendicular to the graphene surface. Figure 9 shows the average order parameter as a function of distance from the graphene surface calculated under each temperature gradient. Under the temperature gradient 1.25 K/nm, the order parameter has a trough at 4 Å and a maximum at 15 Å, respectively. At 4 and 5 Å, the order parameter is about −0.4 and −0.2, respectively, which suggests the cation rings at the bottom of the nano-droplet tend to be parallel to the graphene surface. At 15 Å, the order parameter has a value of 0.65, corresponding to an angle of 60°. In other layers, the order parameter tends to have positive values and the angles are between 30° and 60°, suggesting the cation rings are inclined away from the surface.

It can be observed in Figure 9 that the trough in order parameter appears at the same distance under different temperature gradients. However, the maximum values have different locations. Under temperature gradients 1.25 and 2.5 K/nm, the maxima appear at 15 Å with the values being 0.65 and 0.6, respectively. Under temperature gradients 3.75 and 5 K/nm, the maxima appear at 11 Å and the values are about 0.55. The shift of the maximum locations under different temperature gradients is related to the IL nano-droplet geometry change discussed earlier.

4. Conclusion

Thermal migration is a fundamental phenomenon of significant importance in applications such as lubrication. Ionic liquids have the potential to be lubricants with outstanding performance due to their novel properties. In the current work, the thermal migration of an IL nano-droplet on a graphene surface was studied using non-equilibrium MD simulations. Four temperature gradients were applied to the graphene surface by keeping the two ends of the graphene surface at different temperatures. Migration of the IL nano-droplet was observed under all temperature gradients. It was found that the migration is faster when the temperature gradients are higher. During the migration, the size of the bottom layer of the IL nano-droplet was found to increase as a function of simulation time, suggesting the migration is coupled with spreading the IL nano-droplet on the graphene surface. The ions forming the IL nano-droplet organised themselves in layers parallel to the graphene surface. The nano-droplet migrates on the graphene surface down the temperature gradient in a layer-based motion with the ions in each layer having limited displacement in the direction perpendicular to the graphene surface.

This simulation results provide evidence that the ionic droplet has a layered structure and layer-based motion. It is an interesting question whether the layered structure and layer-based motion on the atomic scale has relationship to the laminar flow at the macroscale.

Acknowledgements

This material is based upon work supported by the National Natural Science Foundation of China (No. 51805252) and China Scholarship Council. EJM and YZ were supported by the Air Force Office of Scientific Research under Contract No. AFOSR FA9550-18-1-0321. Computational resources were provided by the Center for Research Computing (CRC) at the University of Notre Dame.

Disclosure statement

No potential conflict of interest was reported by the author(s).

Funding

This material is based upon work supported by the National Natural Science Foundation of China [grant number 51805252] and China Scholarship Council. EJM and YZ were supported by the Air Force Office of Scientific Research under Contract No. AFOSR FA9550-18-1-0321.

ORCID

Jingqiu Wang http://orcid.org/0000-0002-1714-1657
Yong Zhang http://orcid.org/0000-0003-3988-5961
Xiaolei Wang http://orcid.org/0000-0002-9055-1011
Edward J. Maginn http://orcid.org/0000-0002-6309-1347

References

[1] Roberts EW, Todd MJ. Space and vacuum tribology. Wear. 1990;136:157–167.
[2] Dai Q, Khonsari MM, Shen C, et al. Thermocapillary migration of liquid droplets Induced by a Unidirectional thermal gradient. Langmuir ACS J Surf Colloids. 2016;32:7485–7492.
[3] Whitesides GM. The origins and the future of microfluidics. Nature. 2006;442:368–373.
[4] Pratap V, Moumen N, Subramanian RS. Thermocapillary motion of a liquid drop on a horizontal solid surface. Langmuir ACS J Surf Colloids. 2008;24:5185–5193.
[5] Kataoka DE, Troian SM. Patterning liquid flow on the microscopic scale. Nature. 1999;402:794–797.
[6] Smith MK. Thermocapillary migration of a two-dimensional liquid droplet on a solid surface. J Fluid Mech. 1995;294:209–230.
[7] Karapetsas G, Sahu KC, Sefiane K, et al. Thermocapillary-driven motion of a sessile drop: effect of non-monotonic dependence of surface tension on temperature. Langmuir ACS J Surf Colloids. 2014;30:4310–4321.
[8] Bakli C DSHP, Chakraborty S. Mimicking wettability alterations using temperature gradients for water nanodroplets. Nanoscale. 2017;9:12509–12515.
[9] Dai Q, Huang W, Wang X. Micro-grooves design to modify the thermo-capillary migration of paraffin oil. Meccanica. 2016;52:171–181.

[10] Yoshimitsu Z, Nakajima A, Watanabe T, et al. Effects of surface structure on the hydrophobicity and sliding behavior of water droplets. Langmuir ACS J Surf Colloids. 2002;18:5818–5822.
[11] Karapetsas G, Chamakos NT, Papathanasiou AG. Thermocapillary droplet actuation: effect of solid structure and wettability. Langmuir ACS J Surf Colloids. 2017;33:10838–10850.
[12] Dai Q, Huang W, Wang X. Insights into the influence of additives on the thermal gradient induced migration of lubricant. Lubr Sci. 2017;29:17–29.
[13] Dai Q, Huang W, Wang J, et al. The thermal capillary migration properties and controlling technique of ferrofluids. Proc Inst Mech Eng J J Eng Tribol. 2017;231:1441–1449.
[14] Rajegowda R, Kannam SK, Hartkamp R, et al. Thermophoretic transport of ionic liquid droplets in carbon nanotubes. Nanotechnology. 2017;28:155401.
[15] Becton M, Wang X. Thermal gradients on graphene to drive nanoflake motion. J Chem Theory Comput. 2014;10:722–730.
[16] Lohrasebi A, Neek-Amal M, Ejtehadi MR. Directed motion of C60 on a graphene sheet subjected to a temperature gradient. Phys Rev E. 2011;83:042601.
[17] Foroutan M, Fatemi SM, Esmaeilian F, et al. Contact angle hysteresis and motion behaviors of a water nano-droplet on suspended graphene under temperature gradient. Phys of Fluids. 2018;30:052101.
[18] Foroutan M, Zahedi H, Esmaeilian F. Temperature effects on spreading of water nano-droplet on poly(methyl methacrylate): a molecular dynamics simulation study. J Polym Sci B Polym Phys. 2017;55:1532–1541.
[19] Liu W, Ye C, Gong Q, et al. Tribological performance of room-temperature ionic liquids as lubricant. Tribol Lett. 2002;13:81–85.
[20] Ye C, Liu W, Chen Y, et al. Room-temperature ionic liquids: a novel versatile lubricant. Chem Commun. 2001;2001:2244–2245.
[21] Huang W, Wang X. No migration of ionic liquid under temperature gradient. Colloids Surf A Physicochem Eng Asp. 2016;497:167–170.
[22] Plimpton S. Fast algorithms for short range molecular dynamics. J Comput Phys. 1995;117:1–19.
[23] Wang J, Wolf RM, Caldwell JW, et al. Development and testing of a general amber force field. J Comput Chem. 2004;25:1157–1174.
[24] Bayly CI, Cieplak P, Wendy D C, et al. A well-behaved electrostatic potential based method using charge restraints for deriving atomic charges: the RESP model. J Phys Chem. 1993;97:10269–10280.
[25] Frisch MJ, Trucks GW, Schlegel HB, et al. Gaussian 09, revision E.01. Wallingford (CT): Gaussian; 2016.
[26] Brenner DW, Shenderova OA, Harrison JA, et al. A second-generation reactive empirical bond order (REBO) potential energy expression for hydrocarbons. J Phys Condens Matter. 2002;14:783–802.
[27] Nguyen CT, Kim B. Stress and surface tension analyses of water on graphene-coated copper surfaces. Int J Precis Eng Manuf. 2016;17:503–510.
[28] Batchelor GK. An introduction to fluid mechanics. Cambridge, UK: Cambridge University Press; 2000.
[29] Malali S, Foroutan M. Study of wetting behavior of BMIM+/PF6– ionic liquid on TiO2 (110) surface by molecular dynamics simulation. J Phys Chem C. 2017;121:11226–11233.
[30] Sieffert N, Wipff G. Ordering of imidazolium-based ionic liquids at the α-quartz (001) surface: a molecular dynamics study. J Phys Chem C. 2008;112:19590–19603.